Zoo Biology

WILEY

ZOOBIOLOGY

TECHNICAL REPORT OPEN ACCESS

Radiological Landmarks as an Aid in the Interpretation of Rodent Skull Extra-Oral Projections

Quintin Norval[1,2] | Adrian Tordiffe[3,4] | Gerhard Steenkamp[1,4]

[1]Department of Companion Animal Clinical Studies, Faculty of Veterinary Science, University of Pretoria, Pretoria, South Africa | [2]Department of Dental Sciences, Faculty of Health and Wellness Sciences, Cape Peninsula University of Technology, Cape Town, South Africa | [3]Department of Paraclinical Sciences, Faculty of Veterinary Science, University of Pretoria, Pretoria, South Africa | [4]Centre for Veterinary Wildlife Research, Faculty of Veterinary Science, University of Pretoria, Pretoria, South Africa

Correspondence: Quintin Norval (norvalq@cput.ac.za)

Received: 13 August 2024 | **Revised:** 3 February 2025 | **Accepted:** 25 February 2025

Funding: This research was financed by the developmental fund from the Department of Companion Animal Clinical Studies and AgriSETA bursary (Grant BC24UP-18.1).

Keywords: incisors and cheek teeth | osteology | radiography

ABSTRACT

Knowledge of the radiographic anatomy of rodent skulls is essential for accurately interpreting extra-oral radiographs, a non-invasive diagnostic tool commonly used in veterinary practice. Due to the complexity of the skull and the potential for distortion in two-dimensional views, a systematic evaluation of anatomical structures is necessary. This study identifies the most clinically relevant anatomical landmarks on standard extra-oral radiographic views of the skull and mandible in various rodent species, including a cane rat, two woodchucks, and seven common mole rats. Specimens were evaluated with bone and soft tissue intact, as well as dried skulls, to identify key anatomical features. The findings highlight distinct species-specific variations despite general similarities in skull structure. These landmarks were catalogued to aid veterinary professionals in interpreting rodent radiographs. Improved recognition of these structures enhances diagnostic accuracy, enabling better assessment of normal anatomy and potential pathological conditions in rodent patients.

1 | Introduction

An increasing number of rodent species are kept as pets (Rosen and Jablon 2003; Tamimi et al. 2009; 2020) and knowledge of the basic anatomy of this large and diverse group of mammals is useful in providing appropriate veterinary care (Brown and Donnelly 2012; Brenner et al. 2005). Radiography is a critical diagnostic aid in the clinical evaluation of mineralised anatomical structures (Osofsky and Verstraete 2006; Christine and Estella 2020). Various radiographic modalities are available, where choice depends on the preliminary diagnosis and resources available (Gracis 2008; Villamizar-Martinez and Tsugawa 2022). In general, conventional radiography is more suitable for evaluating teeth, whereas computed tomography (CT) or cone-beam computed tomography (CBCT) is more suitable for assessing distorted peri-oral structures such as the nasal cavity turbinates or tympanic bullae in the head (Capello and Cauduro 2016). Tomography provides a three-dimensional (3D) reconstruction free from the obscurity of overlying structures (Capello and Cauduro 2016), while soft tissues, such as those of the neurocranium or facial musculature, are better examined by magnetic resonance imaging (MRI) (Villamizar-Martinez and Tsugawa 2022).

Structures visible on conventional radiography are primarily the result of the interaction between X-rays and mineralized tissues. These tissues (bone, dentin, enamel, cementum and cartilage), act as high-density barriers that effectively block X-ray photons

Summary

- Identifies key radiological landmarks for interpreting rodent skull extra-oral projections.
- Provides a radiographic reference for accurate veterinary diagnosis.
- Demonstrates anatomical correlations using radiographs and sectioned skulls.
- Enhances pattern recognition in rodent radiography to reduce diagnostic errors.
- Supports veterinary professionals in assessing rodent dental and cranial pathology.

to create correlating radiopacities on radiographs. The greatest mineralised tissue, enamel, appears more radiopaque or radiodense, and the less mineralised tissue, cartilage, appears less radiodense. However, bone can have several appearances, as it is a layered structure comprised of inner trabecular bone that appears more radiolucent and outer cortical bone that appears more radiopaque. For bone to have a distinguishable, less dense appearance on a radiograph, its mineralised content must be reduced by more than 30% (Bender 1997).

Extra-oral radiography is used in small animal dentistry since small intra-oral sensors or plates don't fit inside the oral cavity. However, extra-oral radiography is not the optimal mode for viewing cheek teeth in rodents, as the cheek teeth are minute and a higher spatial resolution can be obtained by intra-oral radiography (Gracis 2008; Capello 2016). The incisor teeth are best viewed in extra-oral head projections, but the cheek teeth can only be evaluated in low resolution since the object needs to be as close as possible to the sensor or plate for optimal image quality. Intra-oral sensors or small plates, placed close to the tooth to be examined, would produce higher-quality images due to the absence of distortion from the contra-lateral side typically seen in extra-oral views. These intra-oral sensors or small plates and the paralleling technique are thus used for cheek teeth where a finer inspection is needed in cases where caries, tooth resorption or periodontal disease is suspected. Specifically, mammography plates should be used in small animals to obtain the best extra-oral radiographic resolution (Capello 2016). Despite this, due to the inherent limitations of conventional radiography in projecting a 3D structure onto a two-dimensional (2D) plane, acquiring multiple views from different angles becomes crucial for reconstructing a comprehensive representation of the interested anatomical region. Typically, these views include laterolateral, right and left latero-oblique, dorsoventral and rostrocaudal views (Gracis 2008; Capello 2016). It is, however, advisable to include a projection where a radiolucent tooth speculum is employed to open the bite of the animal to minimize the overlay of the incisal and occlusal surfaces of the teeth when taking latero-oblique radiographs (Boehmer et al. 2009). For laterolateral projections, correct positioning is achieved by assessing the alignment of the bilateral structures such as the incisor teeth, the tympanic bullae or the margins of the mandible without double images (Capello 2016). Considering these adjustments, a sound anatomical base is required of the species being examined, to interpret rodent extra-oral head radiographs.

Due to specific variations and the abovementioned considerations, checklists help reduce errors in radiographic interpretation (Bruno et al. 2015). Given the vast diversity among rodent species, taxonomists have sought to classify them based on shared characteristics, where one such classification by Tullberg classified rodents into sciurognath and hystricognath groups based on the orientation of the mandible's angular processes (Tullberg 1899; Hautier et al. 2011). While modern systems primarily rely on molecular differences, these earlier classifications, rooted in morphological traits, remain valuable for anatomical studies and discussions. This study aimed to develop a checklist of easily identifiable radiographic landmarks in the heads of three rodent species as representatives of these taxonomic groups. This was achieved by correlating head radiographs with various head sections of three different rodent species and by comparing radiographs with physical head or skull sections to identify useful landmarks that correlate with anatomical features. This landmark checklist can potentially reduce errors in radiographic interpretation, a crucial step in the veterinary care of rodents.

2 | Materials and Methods

Ethics approval for this study was given by the UP-Animal Ethics Committee, REC089-21 and by the Ditsong Museum of National History (DNMNH).

We received one greater cane rat (*Thryonomys swinderianus*) and two woodchuck (*Marmota monax*) heads from the Department of Anatomy and Physiology, Faculty of Veterinary Science, University of Pretoria (UP). Seven common mole rat (*Cryptomys hottentotus*) skulls were received from the DNMNH. The heads and skulls were collected previously for reasons unrelated to this study.

Extra-oral head radiographs were obtained for each common mole rat by exposing the head to laterolateral, dorsoventral, and rostrocaudal projections using a portable X-ray generator (Port X-II, Genoray, Republic of Korea) operating at 2.3 mA and 60KV. Reusable phosphor imaging plates (CR sizes: 4 [5.7 × 7.5 cm] and 5 [5.7 × 9.4 cm], iM3, Ireland, United Kingdom]) were developed by a laser scanner (CR7 Vet image plate X-ray scanner, iM3, Ireland, United Kingdom) and images optimised and stored using the Vet Exam software (iM3, Ireland, United Kingdom). Extra-oral head radiographs were also obtained for the greater cane rat and two woodchucks. The greater cane rat head was used for a laterolateral radiographic projection and the two woodchuck heads for dorsoventral and rostrocaudal projections. Due to the larger size of these species, the extra-oral projections described were performed using an X-ray generator (SG Healthcare Jumong CMP200, SG Healthcare, Republic of Korea) at the diagnostic imaging section at Onderstepoort Veterinary Academic Hospital (OVAH, Soutpan Road, Onderstepoort, South Africa, 0110) on larger phosphor cassettes (Fujifilm Pb IP cassette type CC, 24 cm × 30 cm FCR, Tokyo, Japan). The cassettes were developed on a Fujifilm FCR Profect CS reader, Tokyo, Japan, and all processed images were stored on a laptop in Digital Imaging and Communications in Medicine (DICOM) format. The radiographic images were

converted from DICOM to 8-bit.jpeg images and stored on Google Drive (California, USA).

After obtaining radiographs of the heads, the specimens were sectioned along anatomical planes corresponding to the radiographic projections, providing a physical representation of the internal head structures. The greater cane rat and woodchuck heads were sectioned with a saw and the common mole rat skulls were sectioned with a Dremel 3000 (Bosch Power Tools, Konijnenberg 60, 4825 BD Breda, The Netherlands) fitted with a cut-off wheel (24 mm, 409) and mandrel (402).

3 | Results

On the laterolateral projections, the incisor teeth and their apices were visible (Figure 1). The incisor teeth are a prominent feature of the splanchnocranium (viscerocranium) and have enamel only on the labial side, with the highly calcified layer seen as the most radiopaque part of the tooth (Landmarks B and C, in Figures 1 and 2). The rest of the incisor tooth's mineralised content is comprised of dentin. Rodent incisor teeth have a sharp chisel shape, with the edge sloping from the enamel tip at its apogee to the less mineral-dense dentin lingually (Figure 1). An inner radiolucent line, starting from around the distal alveolar margin, can be traced proximally where it widens into a v-shaped apical bud area (Figure 1). A radiolucent line surrounds the tooth and corresponds to the periodontal ligament (PDL) space (Figure 1). Immediately surrounding the PDL is a slightly more radiodense area, which correlates with the alveolar bone proper or the *lamina dura* (Figure 1). The maxillary incisor tooth is embedded in the maxillary bone and forms part of the lateral wall of the nasal passages (Figure 1). The mandibular incisor tooth comprises most of the volume of the mandible (Landmark D in Figures 1 and 2). The apex of the mandibular tooth can be located distal to the last cheek tooth, close to the condylar head of the mandible. A diastema separates the cheek teeth from the clinical crowns of both the maxillary and mandibular incisor teeth (Figure 1). In the common mole rat, the apices of the maxillary incisor teeth were located caudal to the last cheek teeth, while in the greater cane rat, they were located between the first and last cheek teeth (Figure 1). The cheek teeth can be viewed in the mole rat projection in greater resolution compared to the greater cane rat (Figure 1A vs. 1D), because of the superimposition of the oblique projection. The mandibular condylar head and coronoid processes are overlapped by the tympanic bullae and zygomatic rim (Figure 1).

The nasal turbinates and nasal passages are visible on the laterolateral projection (Figure 1) together with the nasal opening and the tympanic bullae, which are located ventral and caudal to the neurocranium. In the laterolateral and dorsoventral views, they are easily identified as circular structures with finer radiodense septae (Landmark E in Figures 1 and 2). The brain cavity can be divided into the anterior, middle, and posterior cranial fossae (Landmark F in Figures 1 and 2).

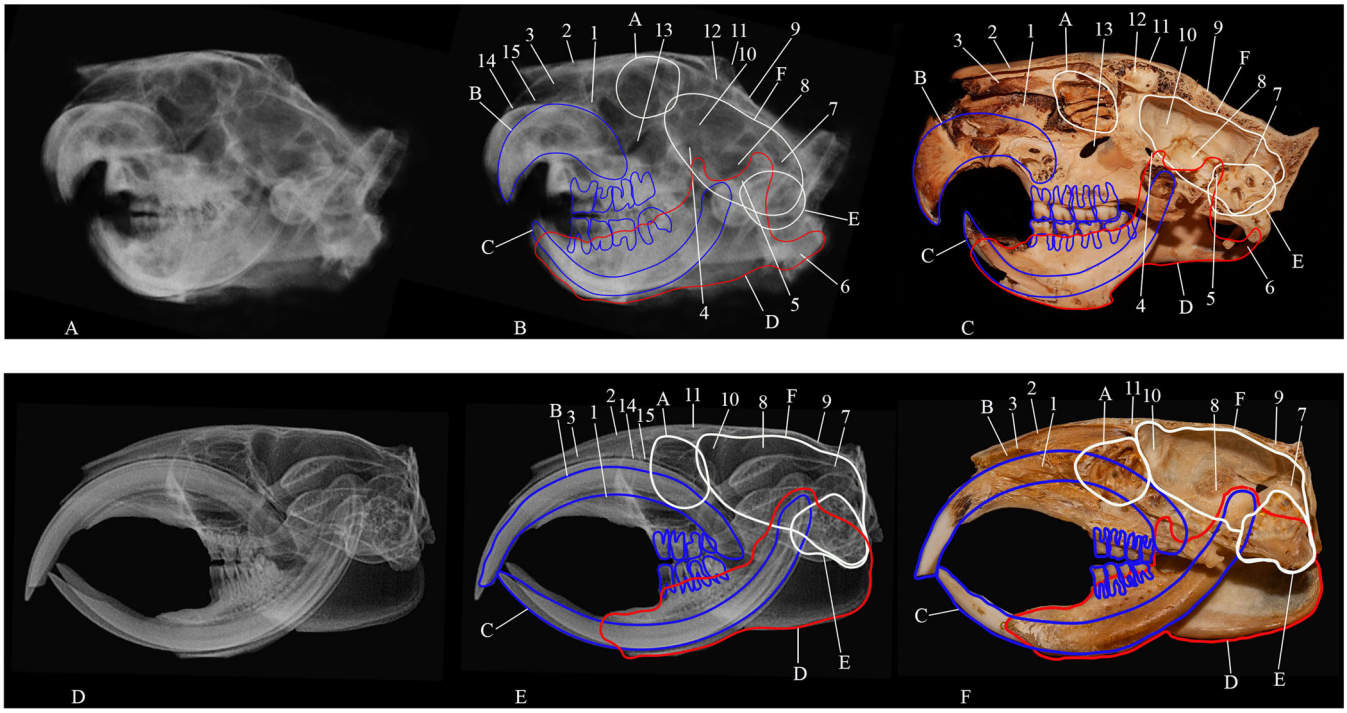

FIGURE 1 | (A–C) From left to right, two laterolateral radiographic projections (oblique offset) of the greater cane rat head and a photo of the mid-sagittal section through the greater cane rat skull. (D–F) From left to right, two laterolateral projections (oblique offset) of a mole rat skull and a photo of a mid-sagittal section through a common mole rat skull. Annotations: A = ethmoid turbinate (*chonchae ethmoidales*), B = maxillary incisor tooth C = mandibular incisor tooth, D = mandible (*mandibula*), E = tympanic bulla (*bulla tympanica*), 1 = maxilloturbinate (*concha nasalis ventralis*), 2 = nasal bone (*os nasale*), 3 = nasoturbinate (*concha nasalis dorsalis*), 4 = *canalis opticus*, 5 = *foramen ovale*, 6 = angular process (*process angularis*), 7 = caudal cranial fossa (*fossa cranii caudalis*), 8 = middle cranial fossa (*fossa cranii medialis*), 9 = parietal (*os parietale*), 10 = rostral cranial fossa (*fossa cranii rostralis*), 11 = frontal bone (*os frontale*), 12 = frontal sinus (*sinus frontale*), 13 = *foramen sphenopalatinum*, 14 = periodontal ligament, 15 = *lamina dura*.

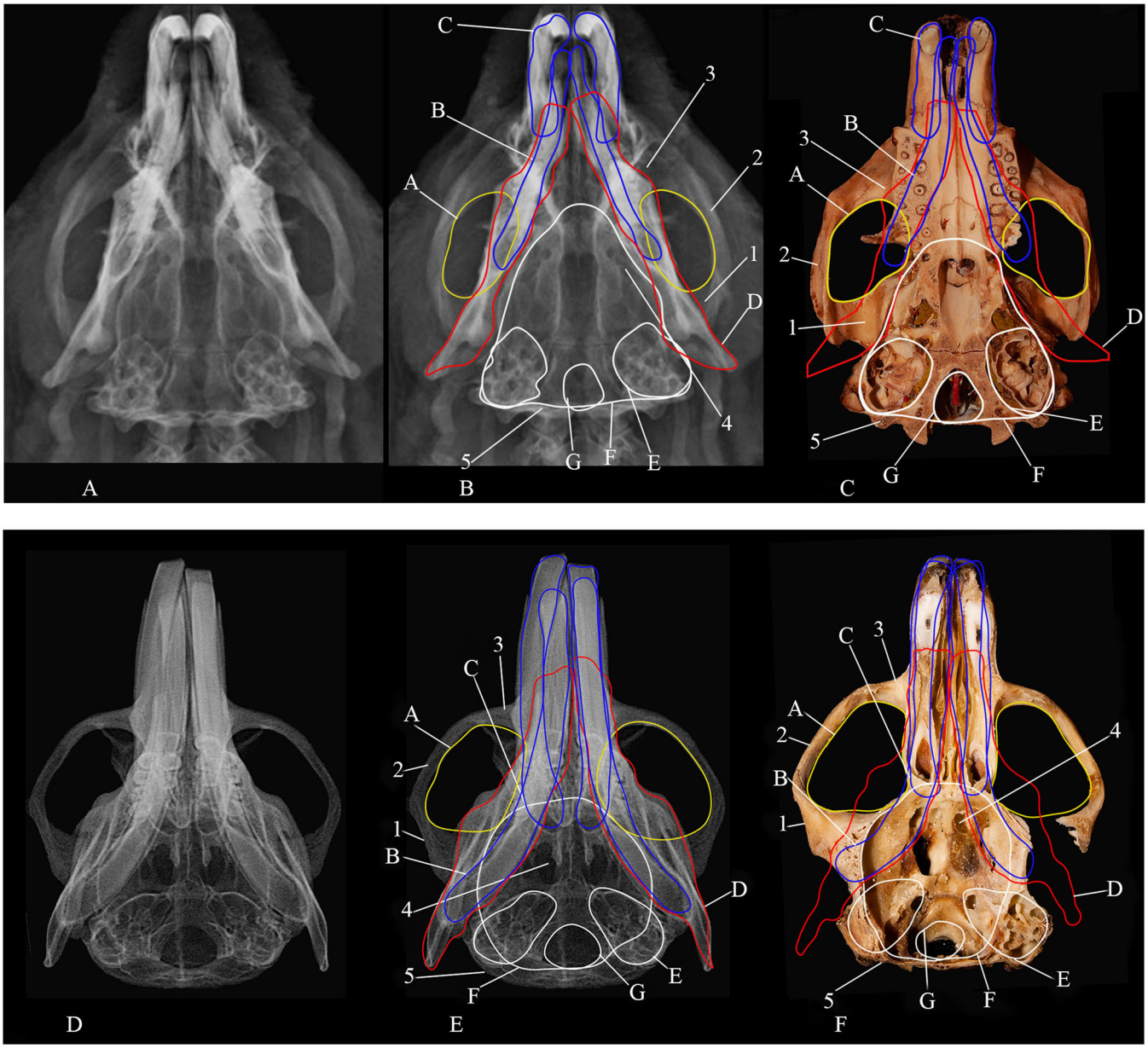

FIGURE 2 | (A–C) From left to right, two dorsoventral radiographic projections of the woodchuck head and a photo of the dorsal section at the level of the hard palate through the woodchuck skull. (D–F) From left to right, two dorsoventral projections of a mole rat skull and a photo of dorsal section at the level of snout through a common mole rat skull. Annotations: A = zygomatic arch foramen, B = mandibular incisor tooth, C = maxillary incisor tooth, D = mandible (*mandibula*), E = tympanic bulla (*bulla tympanica*), F = cranial cavity (*cavum cranii*), G = foramen magnum, 1 = temporal bone (*os temporale*), 2 = zygomatic bone (*os zygomaticum*), 3 = maxilla, 4 = ethmoid foramen (*foramen ethmoidale*), 5 = occipital bone (*os occipital*).

The dorsoventral projection allowed visualisation of the orbits, zygomatic arch, temporomandibular joint (TMJ), tympanic bulla, incisor teeth apices, foramen magnum, oronasal opening, as well as the width of the nasal bone and the patency of the airway allowing for the comparison of bilateral structures (Figure 2). In the dorsoventral radiographic view (Figure 2), the hystricognath rodent mandible has an angular process that is lateral to the plane of the incisor alveolus (e.g., mole rat Figure 2E) and the sciurognath mandible has an incisor alveolus that is aligned to the angular process (e.g., woodchuck in Figure 2B).

The rostrocaudal radiographic view is useful for assessing the patency of the nasal passage, the TMJ and the plane of the occluded cheek teeth (Figure 3). Nasal passages of rodents have intricate conchae or turbinates, which can be divided into the maxilloturbinate, nasoturbinate, and ethmoid turbinates. In this view, they can be seen as circular structures projecting from the lateral nasal wall into the nasal cavity. Notably, the ethmoid turbinates' caudal border correlates to the rostral border of the brain cavity (Landmark A in Figure 1).

4 | Discussion

While experience is important in accurately interpreting radiographs, the literature on identifying consistent landmarks

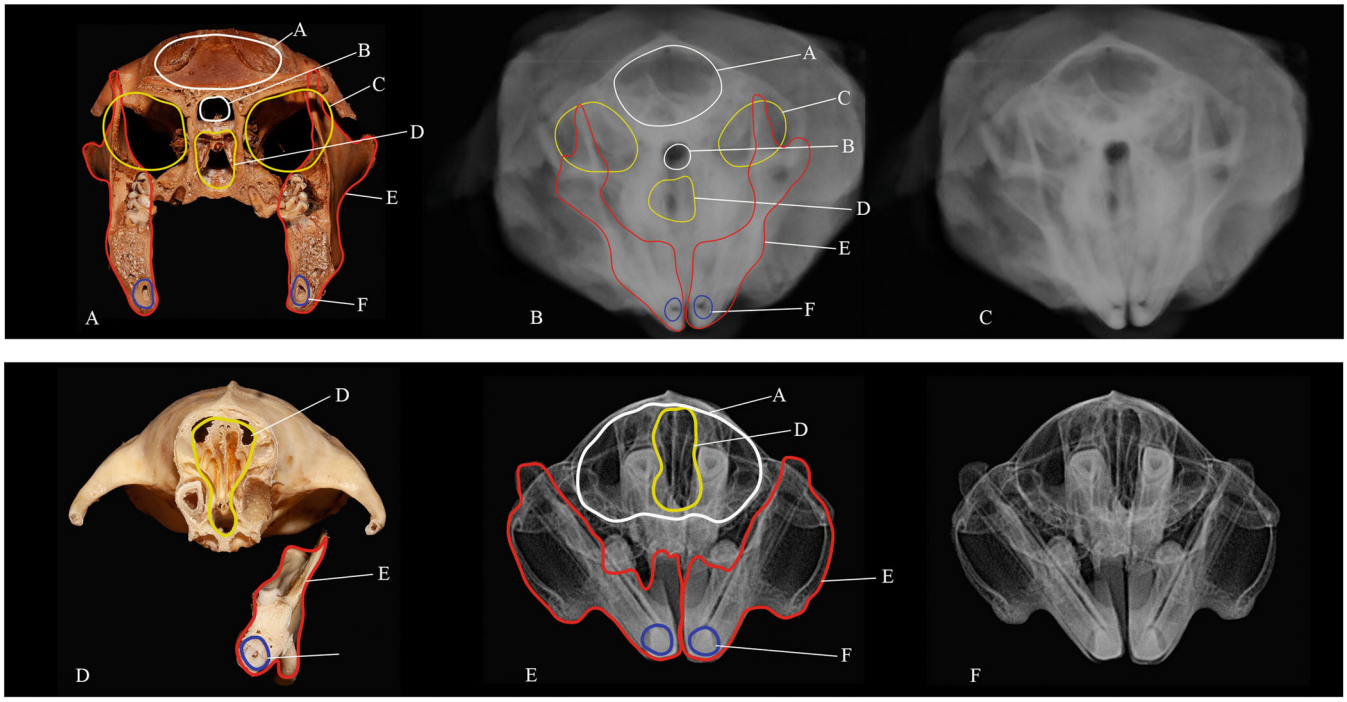

FIGURE 3 | (A–C) From left to right, a photo of a transverse section at the level of the eyes through the woodchuck skull and two rostrocaudal radiographic projections of the same woodchuck head. (D–F) From left to right, a photo of a transverse section at the level of the start of the rostrum through a common mole rat skull and two rostrocaudal radiographic projections of the same skull. Annotations: A = cranial cavity (*cavum cranii*), B = olfactory bulb (*bulbus olfactorius*), C = orbit (*orbita*), D = nasal cavity (*cavum nasi*), E = mandible (mandibula), F = mandibular incisor tooth.

between rodent species is limited. This study expands on current knowledge by presenting a set of easily identifiable radiographic landmarks in the heads of three rodent species. The findings are based on a comparison of radiographs with the physical head sections of these rodents, allowing for a clear correlation between the landmarks and actual anatomical features. However, while anatomical sections represent distinct planes, 2-D radiographic projections overlay all these sections into a single image. Thus, the anatomical sections serve as a physical reference for identifying the internal structures which can be used to develop a standardized checklist to ultimately reduce errors in radiographic interpretation for optimal veterinary care (Christine and Estella 2020; Boehmer et al. 2009). In the future, computer-aided diagnostic systems utilising such checklists, pattern recognition, and large reference databases could automate radiographic interpretation.

This study examined representatives from only two of the three suborders of Rodentia, namely hystricognath and sciuromorph due to a limitation on wet specimen availability. Both greater cane rats and common mole rats are from the hystricognath rodent infraorder, while the woodchucks are classified in the sciuromorph infraorder. To this end, it is important to inspect multiple views, as one projection is not sufficient to properly evaluate an area.

Visible in the laterolateral radiographic projections (Figure 1) both the maxillary and mandibular incisor teeth are curved. The maxillary incisor teeth have an increased curvature (roughly three-eighths of a circle) when compared to the mandibular incisors, which generally form a flatter curve (around a quarter of a circular circumference), as often cited by authors (Gracis 2008; Morris et al. 2019). The length and arc form of these incisor teeth are affected by rodent diet type (abrasiveness) and behaviour, while the more rounded arch of the maxillary incisor tooth is due to the anatomical restrictions of competing vital structures in the skull (Morris et al. 2019). Additionally, in most species, the mandibular incisor tooth generally has a longer rostrocaudal length than its maxillary counterpart. Mole rats, especially the *Georychus* and *Cryptomys* species, are chisel-tooth diggers, in contrast to the *Bathyergidae* mole rats which are scratch diggers (Mcintosh and Cox 2016) and the difference between this tooth usage is clear in Figure 1. The incisor teeth of *Cryptomys* spp. are noticeably longer and exhibit a more mesial procumbency compared to the grass-cutting greater cane rat. This aligns with the general observation that rodents with longer incisors tend to be either subterranean (living underground) or consume more abrasive food sources (Morris et al. 2019).

To evaluate the bone in a laterolateral radiograph, a systematic approach can be followed tracing the outline of the skull from rostral to caudal. Starting at the nasal bone, the most rostrodorsal landmark, move caudal to the frontal bone where the parietal bones can be observed as the dorsal outline of the skull. (Figure 1, nos. 2, 11 and 9). The occipital bone forms the caudodorsal border and moving caudal to rostral and starting at the ventral end of the occipital bone, the temporal, sphenoid, maxilla, and incisive bones can be traced to form the ventral border of the skull on the laterolateral radiographic projection (Figure 1). The outline of the mandible is difficult to follow in the areas of the mandibular angular processes, the coronoids, and the condylar processes of the mandible (D in Figure 1). The

condylar process is in close association with the tympanic bullae, with the coronoid vertical to the last molar tooth. We found that adjusting or toggling the contrast of the images helps to delineate the structures in this difficult-to-interpret region. An obvious and large orientating landmark on a laterolateral radiograph of rodents is the incisor teeth.

The tympanic bullae are easily identifiable as a landmark at the caudal end of the skull base and are characterised by the convoluting circular lines formed by the septae of the tympanic apparatus. The ethmoid turbinates are located rostral to the brain cavity and can be used to orientate other proximate structures, that is, the caudal cranium cavity and the rostral nasal cavity (whole or partial). The ventral surface of the mandible can be traced from rostral to caudal, terminating in an angular process, but the articulating surface on the laterolateral projections is obscured. From these easily identifiable landmarks, a radiographer can orientate other anatomical structures and interpret a radiograph.

Dorsoventral radiographs allow visualisation of the cranial bones in a horizontal dimension and can be divided into two lateral sections that form the zygomatic arch and the bones positioned between the arches. The central cranial bones viewed dorsally and moving from rostral to caudal, include the incisive, maxilla, palatine, sphenoid, temporal, and occipital bones. The zygomatic arch foramina (marked A in Figure 2) are formed by three bones, from rostral to caudal: the maxilla, zygomatic, and temporal bones. Finally, the dorsoventral radiograph is very useful for comparing bilateral overlapping structures such as the tympanic bullae, the shape of the mandible, the shape of the incisor teeth and their apices as well as the zygomatic arches.

In both dorsoventral and laterolateral radiographic projections, a key area of interest is the nasal cavity and its relationship to the apices of the maxillary incisor teeth. In different rodent species, the apex of the maxillary incisor tooth can terminate anywhere within the diastema area or even as far back as distal to the last cheek tooth (Figure 1, greater cane rat vs. common mole rat). The width of the nasal bone can be effectively assessed from the dorsoventral radiographic projection. The rostrocaudal view is useful for evaluating the TMJ, an area that is unclear on the laterolateral view and the nasal conchae can be seen in cross-section in this view. The rostrocaudal view is used to provide a different perspective and augment a holistic picture in combination with the laterolateral and dorsoventral projections.

In conclusion, this study highlights the importance of systematic radiograph evaluation in diagnosing and planning the treatment of head and tooth conditions in small mammals, particularly rodents. By correlating radiographs from three different head projections with sectioned skulls, we were able to identify key anatomical landmarks. This improved understanding of rodent head anatomy through radiography will be of significant clinical benefit to veterinarians dealing with small mammals.

Author Contributions

Quintin Norval: concept and design, acquisition of data, analysis and interpretation of data, drafting article, final approval of completed article, agreement to be accountable. **Gerhard Steenkamp:** concept and design, analysis and interpretation of data, reviewing article (not mentioned anywhere), final approval of completed article, agreement to be accountable. **Adrian Tordiffe:** concept and design, analysis and interpretation of data, drafting article, final approval of completed article, agreement to be accountable.

Acknowledgments

Prof. Martina Crole for help with the anatomy of the greater cane rat and Ms Wilma Olivier for the greater cane rat and woodchuck specimens from the Department of Anatomy and Physiology, Faculty of Veterinary Science, UP. The author would like to thank Dr Teresa Kearney (Vertebrate Department, Small Mammals, DNMNH) for the mole rat skulls. This research was financed by the developmental fund from the Department of Companion Animal Clinical Studies and AgriSETA bursary (Grant BC24UP-18.1).

Conflicts of Interest

The authors declare no conflicts of interest.

Data Availability Statement

The data that support the findings of this study are available on request from the corresponding author. The data are not publicly available due to privacy or ethical restrictions.

References

Bender, I. B. 1997. "Factors Influencing the Radiographic Appearance of Bony Lesions." *Journal of Endodontics* 23, no. 1: 5–14.

Boehmer, E., E. Böhmer, Z. Brenner, et al. 2009. "Objective Interpretation of Dental Disease in Rabbits, Guinea Pigs and Chinchillas: Use of Anatomical Reference Lines." *Tierarztl Prax Ausg K Kleintiere Heimtiere* 37, no. 04: 250–260.

Brenner, S. Z. G., M. G. Hawkins, L. A. Tell, W. J. Hornof, C. G. Plopper, and F. M. Verstraete. 2005. "Clinical Anatomy, Radiography, and Computed Tomography of the Chinchilla Skull." *Comp Cont Education Practice* 27, no. 12: 933–943.

Brown, C., and T. M. Donnelly. 2012. "Disease Problems of Small Rodents." *Ferrets, Rabbits, and Rodents*: 354–372. https://doi.org/10.1016/b978-1-4160-6621-7.00027-0.

Bruno, M. A., E. A. Walker, and H. H. Abujudeh. 2015. "Understanding and Confronting Our Mistakes: The Epidemiology of Error in Radiology and Strategies for Error Reduction." *Radiographics* 35, no. 6: 1668–1676.

Capello, V. 2016. "Diagnostic Imaging of Dental Disease in Pet Rabbits and Rodents." *Veterinary Clinics of North America: Exotic Animal Practice* 19, no. 3: 757–782.

Capello, V., and A. Cauduro. 2016. "Comparison of Diagnostic Consistency and Diagnostic Accuracy Between Survey Radiography and Computed Tomography of the Skull in 30 Rabbits With Dental Disease." *Journal of Exotic Pet Medicine* 25, no. 2: 115–127.

Christine, B., and B. Estella. 2020. "Skull Shape Diversity in Pet Rabbits and the Applicability of Anatomical Reference Lines for Objective Interpretation of Dental Disease." *Veterinary Sciences* 7, no. 4: 182.

Gracis, M. 2008. "Clinical Technique: Normal Dental Radiography of Rabbits, Guinea Pigs, and Chinchillas." *Journal of Exotic Pet Medicine* 17, no. 2: 78–86.

Hautier, L., R. Lebrun, S. Saksiri, J. Michaux, M. Vianey-Liaud, and L. Marivaux. 2011. "Hystricognathy vs Sciurognathy in the Rodent Jaw: A New Morphometric Assessment of Hystricognathy Applied to the Living Fossil Laonastes (Diatomyidae)." *PLoS One* 6, no. 4: e18698.

Mcintosh, A. F., and P. G. Cox. 2016. "Functional Implications of Craniomandibular Morphology in African Mole-Rats (Rodentia: Bathyergidae)." *Biological Journal of the Linnean Society* 117, no. 3: 447–462.

Morris, P. J. R., P. G. Cox, and S. N. Cobb. 2019. “Mechanical Significance of Morphological Variation in Diprotodont Incisors.” *Royal Society Open Science* 6, no. 3: 181317.

Osofsky, A., and F. J. M. Verstraete. 2006. “Dentistry in Pet Rodents.” *Compendium of Continuing Education in Practice* 28, no. 1: 61–73.

Rosen, T., and J. Jablon. 2003. “Infectious Threats From Exotic Pets: Dermatological Implications.” *Dermatologic Clinics* 21, no. 2: 229–236.

Tamimi, N. S., T. Bahare, J. Shahram, and R. Amir. 2020. “A Retrospective Study on 1587 Exotic Pets Presented to the Small Animal Veterinary Hospital, University of Tehran. Iraqi.” *Journal of Veterinary Medicine* 44, no. E0: 1–6.

Tullberg, T. 1899. Ueber das System der Nagethiere: eine phylogenetische Studie / von Tycho Tullberg. https://doi.org/10.5962/bhl.title.1733.

Villamizar-Martinez, L. A., and A. J. Tsugawa. 2022. “Diagnostic Imaging of Oral and Maxillofacial Anatomy and Pathology.” *Veterinary Clinics of North America: Small Animal Practice* 52: 67–105.